Title

The C-Terminal End of HIV-1 Vpu Has a Clade-Specific Determinant That Antagonizes BST-2 and Facilitates Virion Release.

Journal

Journal of Virology, 93(11)

ISSN

0022-538X

Authors

Sharma, Shilpi
Jafari, Moein
Bangar, Amandip
et al.

Publication Date

2019-06-01

DOI

10.1128/jvi.02315-18

Peer reviewed

AMERICAN SOCIETY FOR MICROBIOLOGY | Journal of Virology®

VIRUS-CELL INTERACTIONS

The C-Terminal End of HIV-1 Vpu Has a Clade-Specific Determinant That Antagonizes BST-2 and Facilitates Virion Release

Shilpi Sharma,[a] Moein Jafari,[a] Amandip Bangar,[a] Karen William,[a] John Guatelli,[a,b] Mary K. Lewinski[a,b]

[a]Department of Medicine, University of California San Diego, La Jolla, California, USA
[b]VA San Diego Healthcare System, San Diego, California, USA

ABSTRACT The cellular protein bone marrow stromal antigen-2 (BST-2)/tetherin acts against a variety of enveloped viruses by restricting their release from the plasma membrane. The HIV-1 accessory protein Vpu counteracts BST-2 by downregulating it from the cell surface and displacing it from virion assembly sites. Previous comparisons of Vpus from transmitted/founder viruses and between viruses isolated during acute and chronic infection led to the identification of a tryptophan at position 76 in Vpu (W76) as a key determinant for the displacement of BST-2 from virion assembly sites. Although present in Vpus from clades B, D, and G, W76 is absent from Vpus from clades A, C, and H. Mutagenesis of the C-terminal region of Vpu from two clade C viruses led to the identification of a conserved LL sequence that is functionally analogous to W76 of clade B. Alanine substitution of these leucines partially impaired virion release. This impairment was even greater when the mutations were combined with mutations of the Vpu β-TrCP binding site, resulting in Vpu proteins that induced high surface levels of BST-2 and reduced the efficiency of virion release to less than that of virus lacking *vpu*. Microscopy confirmed that these C-terminal leucines in clade C Vpu, like W76 in clade B, contribute to virion release by supporting the displacement of BST-2 from virion assembly sites. These results suggest that although encoded differently, the ability of Vpu to displace BST-2 from sites of virion assembly on the plasma membrane is evolutionarily conserved among clade B and C HIV-1 isolates.

IMPORTANCE Although targeted by a variety of restriction mechanisms, HIV-1 establishes chronic infection in most cases, in part due to the counteraction of these host defenses by viral accessory proteins. Using conserved motifs, the accessory proteins exploit the cellular machinery to degrade or mistraffic host restriction factors, thereby counteracting them. The Vpu protein counteracts the virion-tethering factor BST-2 in part by displacing it from virion assembly sites along the plasma membrane, but a previously identified determinant of that activity is clade specific at the level of protein sequence and not found in the clade C viruses that dominate the pandemic. Here, we show that clade C Vpu provides this activity via a leucine-containing sequence rather than the tryptophan-containing sequence found in clade B Vpu. This difference seems likely to reflect the different evolutionary paths taken by clade B and clade C HIV-1 in human populations.

KEYWORDS BST-2, Vpu, host-pathogen interactions, human immunodeficiency virus, molecular biology, restriction factors, virology, virus-host interactions

A variety of host restriction factors have evolved as a first line of innate defense against viral pathogens. In the case of primate lentiviruses, these host factors include the APOBECs, TRIM5α, SAMHD1, the SERINCs, and BST-2 (bone marrow stromal antigen-2). APOBEC proteins introduce hypermutations in human immunodeficiency virus type 1

Citation Sharma S, Jafari M, Bangar A, William K, Guatelli J, Lewinski MK. 2019. The C-terminal end of HIV-1 Vpu has a clade-specific determinant that antagonizes BST-2 and facilitates virion release. J Virol 93:e02315-18. https://doi.org/10.1128/JVI.02315-18.

Editor Wesley I. Sundquist, University of Utah

Address correspondence to John Guatelli, jguatelli@ucsd.edu, or Mary K. Lewinski, mlewinski@ucsd.edu.

Received 28 December 2018
Accepted 6 March 2019
Accepted manuscript posted online 13 March 2019
Published 15 May 2019

(HIV-1) reverse transcripts (1); TRIM5α destabilizes the capsid, thereby inhibiting reverse transcription (2, 3); SAMHD1 depletes the intracellular pool of deoxynucleoside triphosphates (dNTPs) to block reverse transcription (4–8); SERINCs inhibit the infectivity of progeny virions (9, 10); and BST-2 inhibits virion release by tethering virions to the cell surface (11, 12).

Constitutively expressed in certain cell types (B and T cells, plasmacytoid dendritic cells, myeloid cells, and many transformed cell lines) and interferon inducible in others, BST-2 (also known as tetherin, CD317, and HM1.24) is a type II transmembrane protein with an unusual topology that enables it to trap newly formed enveloped virions on cellular membranes (11, 12). BST-2 has a short N-terminal cytoplasmic domain, a transmembrane domain, an α-helical ectodomain, and a C-terminal glycosylphosphatidylinositol (GPI) membrane anchor. Like other GPI-modified proteins, BST-2 localizes to lipid rafts (13), which are also the budding sites of HIV virions (14). The BST-2 ectodomain dimerizes to form a rigid coiled-coil region that keeps the transmembrane and GPI membrane anchors separated such that one can partition into the budding virion while the other remains in the plasma membrane, thereby forming a virion-cell tether. The virion-tethering activity of BST-2 is not specific to HIV; BST-2 restricts the release of several enveloped viruses, including all retroviruses tested so far, arenaviruses (Lassa virus), filoviruses (Ebola and Marburg virus-like particles]), and Kaposi's sarcoma-associated herpes virus (KSHV) (11, 12, 15–18). In addition to its activity as a restriction factor, BST-2 induces NF-κB activity in response to viral infection and consequently proinflammatory signaling; this activity may or may not be linked to its tethering activity (19, 20). BST-2 also seems important for the development of antiviral cell-mediated immunity, which might be a consequence of a role in the degradation of viral proteins or the display of viral peptides by major histocompatibility complex class II (21). To keep pace with their hosts, viruses have evolved specific antagonists of BST-2. These include the Env glycoprotein of HIV-2 (22, 23), Nef of simian immunodeficiency virus (SIV) (24, 25), the Ebola glycoprotein (16), the K5 protein of KSHV (17, 26), and Vpu of HIV-1 (11, 12).

The BST-2 antagonist Vpu is unique to HIV-1 and its primate lentiviral predecessors. Vpu is a short, oligomeric, type I integral transmembrane protein. Its cytoplasmic domain can be subdivided structurally into α-helices 1 and 2, which are separated by a hinge region (27, 28). The hinge region contains two conserved serines that are phosphorylated by casein kinase II and form a DSGxxS β-TrCP recognition motif (29–31). When Vpu interacts with its targets (in the case of BST-2, via the two proteins' transmembrane domains), the phosphorylated DSGxxS sequence recruits β-TrCP, a substrate adaptor for an SCF (Skp1/Cullin/F-Box protein) E3 ubiquitin ligase complex. Via this interaction, Vpu induces the ubiquitination and subsequent degradation and mistrafficking of cellular proteins, including CD4 and BST-2 (32–37). However, mutants of the β-TrCP binding motif in Vpu are only partially impaired in counteracting BST-2-mediated restriction of virion release.

In addition to targeting BST-2 for ubiquitination and degradation, Vpu inhibits newly synthesized BST-2 from reaching the cell surface (38), and it inhibits the recycling of endocytosed BST-2 (39, 40). In addition to binding the SCF E3 ligase complex, the DSGxxS motif of Vpu also binds to the clathrin adaptor protein complexes AP-1 and AP-2 in cooperation with an acidic leucine-based motif (ExxxLV) in helix 2 (41, 42). These interactions contribute to the downregulation of BST-2 from the cell surface and its sequestration in a perinuclear compartment (42–45).

Moreover, several lines of evidence suggest that the degradation and downregulation of BST-2 is only weakly correlated with Vpu's ability to enhance virion release (46–48). As noted above, a Vpu hinge-serine mutant unable to bind β-TrCP retains partial activity in enhancing virion release, even though it is unable to downregulate BST-2 (47). This partial activity was explained by the displacement of BST-2 from virions (Gag) in the plane of the plasma membrane, an activity independent of the hinge region phosphoserines and of BST-2 downregulation and that mapped to Vpu cytoplasmic helix 2 (47). Conversely, while characterizing Vpus from inferred transmitted/founder viruses and while comparing Vpus cloned from longitudinally collected plasma

FIG 1 C-terminal region of Vpu is relatively variable. (A) A multiple-sequence alignment of Vpu proteins from various clades of HIV-1, generated using Clustal-Omega (EMBL) software. Shown are the consensus sequences from the indicated clades from the LANL database (51). The conserved β-TrCP-binding phosphoserines are boxed in red, and the location of the conserved tryptophan (W76) in clades B, D, and G is indicated by the red arrow. (B) Sequence alignment of HIV-1 Vpu proteins from MJ4 (infectious molecular clone of clade C HIV-1, used in this study) and NL4-3 (representative of clade B).

from patients during the acute and chronic phases of infection, we identified clade B Vpus that were impaired for enhancing virion release yet were able to downregulate BST-2 and CD4 (49). The defect in these Vpus mapped to a W76G polymorphism near their C termini. We used immunofluorescence microscopy to support the hypothesis that W76, like helix 2, is required for the displacement of BST-2 from Gag. Using nuclear magnetic resonance (NMR) spectroscopy, we found that the C terminus of Vpu and particularly W76 interacted with and inserted into lipids, leading to a model in which W76 anchors the C terminus to the plasma membrane and enables Vpu to displace BST-2 from virion assembly sites (50). Remarkably, W76, while well conserved in clade B, D, and G Vpu proteins, is absent from clades A, C, and H.

Here, we address the question of whether clade C Vpu encodes BST-2 displacement activity and, if so, by what means. We identify a short motif containing two adjacent leucine residues in the C terminus of clade C Vpu that is functionally analogous to W76 of clade B. These leucines contribute to the displacement effect, and when they are mutated together with the hinge region phosphoserines, Vpu-mediated enhancement of virion release is lost.

RESULTS

Vpu proteins differ in their C-terminal regions. Figure 1A shows a sequence alignment of the consensus sequences of Vpu from various clades. All the sequences were obtained from the Los Alamos National Laboratory (http://www.hiv.lanl.gov/) (51). The Vpu proteins from the various clades share about 35% sequence identity, with a high degree of similarity in the transmembrane (TM) region, helix 1, and the hinge region. Helical region 2 and the C terminus are more variable. Vpu enhances virion release by downregulating BST-2 from the cell surface and by displacing BST-2 from virion assembly sites (47, 50). The tryptophan at position 76 in helix 2 was previously identified in clade B as essential for the BST-2 displacement phenomenon (49, 50), but

while this tryptophan residue is well conserved in clades B, D, and G, it is absent from clades A, C, and H. W76 is part of the conserved sequence HAPW in clades B and D. The sequence in clade C Vpu that aligns with the HAPW sequence of clade B Vpu is LRLL, as shown in Fig. 1A. The entire LRLL sequence is highly conserved in clade C, with prior studies noting that it was lacking in only 6 out of 115 subtype C viruses surveyed (52, 53).

The diphosphoserine β-TrCP-binding motif of clade C Vpu does not fully account for the enhancement of virion release. For clade B Vpu, the conserved diphosphoserine motif in the hinge region is the major driver of BST-2 degradation and downregulation, but this motif and these processes do not fully account for the enhancement of virion release (36, 37, 48). Phosphoserine mutants retain partial activity with respect to virion release, and this has been attributed to Vpu's ability to displace BST-2 from virion assembly sites (47). Therefore, we first evaluated whether or not the phosphoserines of clade C Vpu behave similarly to those of clade B. To do so, we measured residual virion release enhancement activity when the serines were replaced with asparagines. We used pMJ4, an HIV-1 clade C chimeric infectious molecular clone, for these studies (54). Figure 1B shows an alignment of the clade C MJ4 and clade B NL4-3 Vpu proteins, showing the clade-specific differences between the two proteins in their C termini. We first made a *vpu*-negative construct (pMJ4ΔVpu) by inserting termination codons in place of residues 10 and 13. To complement the MJ4ΔVpu provirus with Vpu in *trans*, we cloned the *vpu* coding sequence from pMJ4 into a pcDNA3.1(−)-based (Invitrogen) plasmid with a Rev response element (RRE) downstream of the cloning site, pcDNA-RRE (49), adding a FLAG epitope tag to the C terminus. To create the β-TrCP-binding mutant of MJ4 Vpu, the two serines at positions 58 and 62 were replaced with asparagines (S58N and S62N; here referred as S58,62N). HeLa P4-R5 cells, which constitutively express BST-2, were transfected with pMJ4ΔVpu, either alone or in combination with plasmids expressing either wild-type MJ4-Vpu or the β-TrCP-binding mutant S58,62N. The next day, the cells were stained for surface BST-2 and intracellular Gag to evaluate BST-2 downregulation, while the released virions were pelleted through a 20% sucrose cushion and quantified by p24 enzyme-linked immunosorbent assay (ELISA). As seen in Fig. 2A, the expression construct encoding wild-type MJ4-Vpu *trans*-complemented the MJ4ΔVpu genome, enhancing the release of virions by over 6-fold (comparing the first and second bars). The S58,62N mutant, in contrast, enhanced the release of virions only about 3-fold. These data recapitulate the previously reported phenotypes of mutants of the clade B Vpu β-TrCP-binding motif. Also similar to clade B Vpu, whereas the wild-type clade C Vpu downregulated BST-2 from the cell surface, the S58,62N mutant did not (Fig. 2B). These differences were not due to differential expression of the Vpu proteins; as seen in Fig. 2C, the S58,62N mutant was better expressed than the wild type, despite its impaired activity. The ability of the β-TrCP binding site mutant to enhance virion release indicated the presence of additional determinants in clade C Vpu that contribute to the antagonism of BST-2-mediated restriction.

The C terminus of clade C Vpu has determinants that support the enhancement of virion release. We studied the $_{78}$LRLL$_{81}$ region of the clade C Vpu C terminus, since, as noted above, this region aligns with the $_{73}$HAPW$_{76}$ region of clade B Vpu (Fig. 1B). The sequence of MJ4 Vpu, highlighting the positions of the two phosphorylated serines and the C-terminal residues that we mutated, is shown in Fig. 2D. The various mutants and their activity with respect to enhancing virion release and downregulating BST-2 from the cell surface are summarized in Table 1. First, we made single, double, and quadruple mutants of the $_{78}$LRLL$_{81}$ residues, replacing these residues with alanines. These mutants were then expressed in HeLa P4-R5 cells along with the *vpu*-negative proviral clone of MJ4, pMJ4ΔVpu, and their activity was assessed compared to that of wild-type Vpu. First, we measured the ability of these mutants to enhance virion release. As seen in Fig. 3A, all the mutants were able to enhance virion release, albeit to different extents and in some cases significantly less effectively than wild-type Vpu.

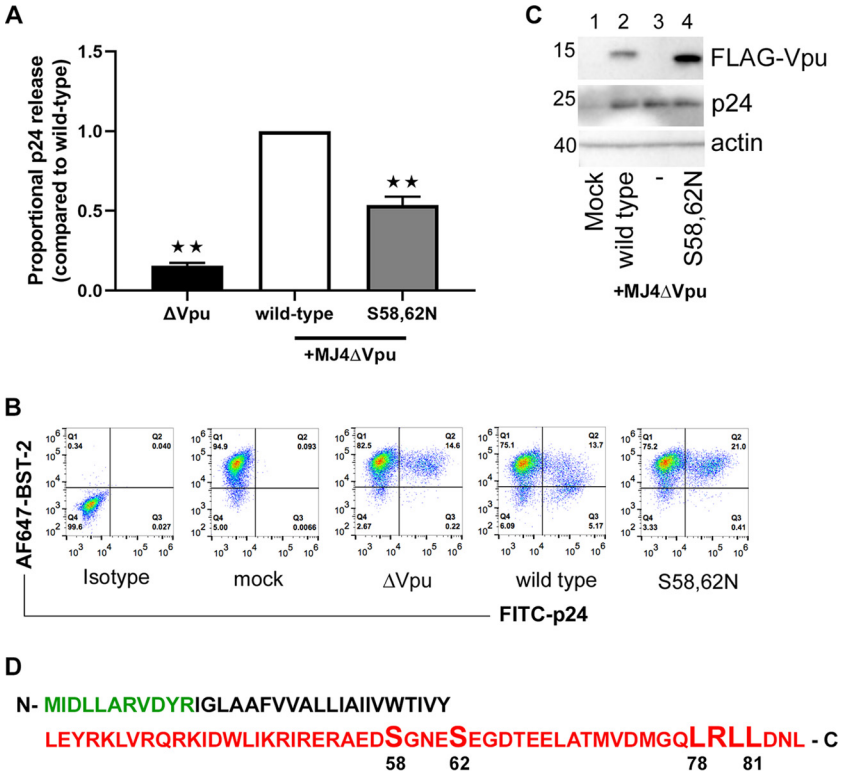

FIG 2 Clade C Vpu-S58,62N retains partial activity at enhancing virion release despite its inability to downregulate BST-2. (A) HeLa P4-R5 cells were transfected with proviral MJ4ΔVpu plasmid with empty vector or in combination with expression constructs of wild-type Vpu or the β-TrCP-binding mutant Vpu-S58,62N in duplicate. The next day, the supernates were harvested and pelleted over 20% sucrose cushions and then evaluated for Gag content by p24 ELISA. Ratio paired *t* test, compared to results for wild-type Vpu, was performed on unnormalized data from three independent experiments using GraphPad Prism (version 7.0c). **, $P < 0.01$. Error bars are standard deviations. (B) The cells from a representative experiment shown in panel A were harvested and stained for cell surface BST-2 expression using Alexa Fluor 647-conjugated mouse anti-BST-2 antibody and then permeabilized and stained with FITC-conjugated mouse anti-Gag p24 antibody. The cells were fixed after staining and analyzed by flow cytometry using FlowJo software. (C) The whole-cell lysates were blotted for the expression of Vpu proteins using mouse anti-FLAG antibody, Gag p24 with mouse anti-HIV-1 *gag*, and anti-actin as a loading control. This immunoblot is representative of three independent experiments. (D) The amino acid sequence of MJ4 Vpu highlighting the serines and the C-terminal residues (large font) which were mutated for this study. The extracellular region is in green, the TM domain is in black, and the cytoplasmic tail is in red.

The β-TrCP binding site mutant (S58,62N) was again significantly but incompletely impaired. Mutants of the LRLL sequence had variable phenotypes but supported the hypothesis that this region contributes to virion release: the L78A, L80A, LL80,81AA, and LRLL78-81AAAA mutants each were significantly impaired for virion release, although the LR78,79AA mutant was not. We also replaced the LRLL region of clade C Vpu with the HAPW sequence from clade B Vpu; this swap mutant was slightly impaired but not statistically different from the wild type. These results suggest that the leucine residues, particularly L80 and L81, contribute to the enhancement of virion release. We next measured the ability of these mutants to downregulate BST-2 from the cell surface. The cells used for the virion release assays were stained with Alexa Fluor 647-conjugated anti-BST-2 antibody, permeabilized, and stained with fluorescein isothiocyanate (FITC)-conjugated anti-Gag p24 antibody. We gated on Gag-positive cells to measure the effects of the various Vpu mutants on BST-2 at the cell surface. As seen from the graph in Fig. 3B and the two-color plots in Fig. 3C, all mutants of one or more of the LRLL residues downregulated BST-2 similarly to wild-type Vpu, indicating that their defect in virion release was not due to impaired BST-2 downregulation. Figure 3B shows the mean fluorescence intensities (MFIs) of the

TABLE 1 Summary of clade C Vpu mutants with respect to their ability to enhance virion release and downregulate BST-2

β-TrCP binding site		*P* value for impairment in virion release vs wild-type Vpu[a]	Ability to downregulate BST-2 vs ΔVpu
Intact	Mutated		
L78A		<0.05	Yes
R79A		NS	Yes
L80A		<0.05	Yes
L81A		NS	Yes
LR/AA		NS	Yes
LL/AA		<0.05	Yes
LRLL/AAAA		<0.05	Yes
LRLL/HAPW		NS	Yes
	S58,62N	<0.05	No
	L78A + S58,62N	NS	No
	R79A + S58,62N	<0.05	No
	L80A + S58,62N	<0.05	No
	L81A + S58,62N	<0.01	No
	LR/AA + S58,62N	<0.01	No
	LL/AA + S58,62N	<0.01	No
	LRLL/AAAA + S58,62N	<0.01	No
	LRLL/HAPW + S58,62N	<0.05	No

[a]NS, not significant.

BST-2 surface stain in the presence of these Vpu proteins compared to when Vpu was absent (ΔVpu) and confirms that the activities of the $_{78}$LRLL$_{81}$ region mutants are similar to that of the wild type. To ensure that the differences in virion release were not due to the differences in the expression of the mutants or to variability of the transfections, we measured the expression of the Vpu proteins by immunoblotting for FLAG (Vpu) and Gag (p55 and p24). As shown in Fig. 3D, all of the Vpu mutants were expressed at least as well as the wild type. Thus, we conclude that the $_{78}$LRLL$_{81}$ region, and more specifically residues L80 and L81, significantly contribute to virion release, even though this region is dispensable for the downregulation of BST-2 from the cell surface.

For clade B Vpu, mutation of W76, like mutation of the β-TrCP binding site, only partially impairs virion release enhancement, but the combination of these mutations renders Vpu inactive (49, 50). Therefore, we made similar combination mutants of clade C Vpu and tested them for their ability to enhance virion release and downregulate BST-2. When combined with mutation of the β-TrCP binding site, C-terminal mutations within the $_{78}$LRLL$_{81}$ region rendered Vpu inactive (Fig. 4A to C); in particular, the single-residue substitutions L80A and L81A drastically impaired virion release when combined with mutations at the β-TrCP binding site (Fig. 4A, L80A+S58,62N and L81A+S58,62N). Paradoxically, virion release was lower in the presence of these mutants than when no Vpu was expressed (ΔVpu). The same phenotype was observed when mutations of both L80 and L81 were combined with mutations of the β-TrCP binding site (LL/AA+S58,62N) or when mutation of the entire $_{78}$LRLL$_{81}$ sequence was combined with mutations of the β-TrCP binding site (LRLL/AAAA+S58,62N). That these combination mutants would support less efficient virion release than the no Vpu condition was surprising. However, measurement of surface BST-2 provided a potential explanation: not only were these mutants unable to downregulate BST-2, their expression increased cell surface BST-2 to more than that of the no Vpu condition (Fig. 4B and C). Western blotting of the cell lysates confirmed that the expression levels of the Vpu mutants were similar (Fig. 4D). Overall, the data indicate that L80 and L81 of clade C Vpu are substantial contributors to virion release and that when these leucines are mutated in combination with the serines of the β-TrCP binding site, Vpu's ability to enhance virion release is lost.

To confirm that these findings were a general feature of clade C Vpus, we cloned and tested Vpu from a primary clade C isolate from early infection, clone

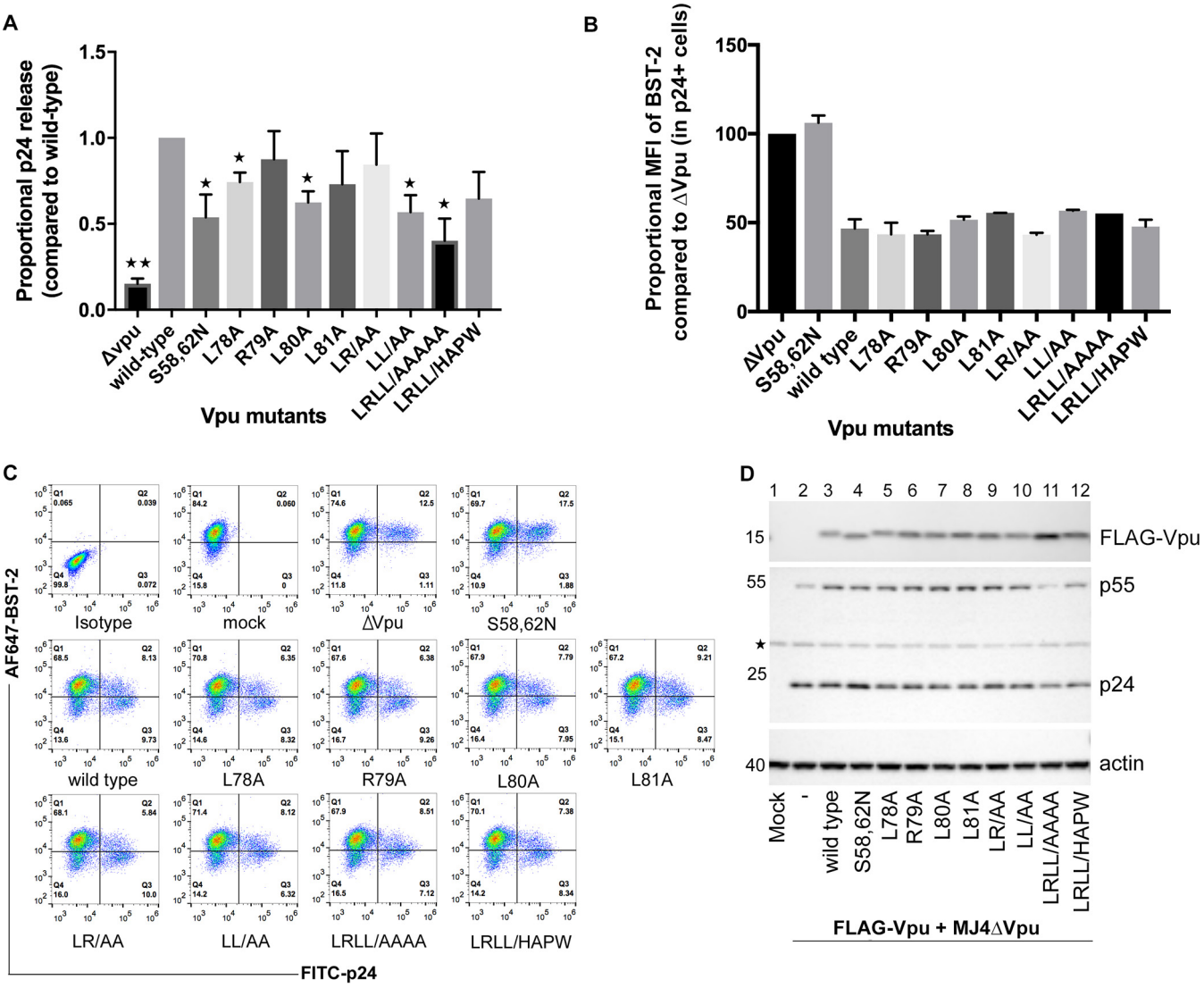

FIG 3 Characterization of C-terminal mutants of clade C Vpu. (A) Vpu mutants were analyzed for their ability to enhance virion release by measuring the concentration of pelletable p24 antigen in the supernate by p24 ELISA in duplicate. Ratio paired *t* test, compared to data for wild-type Vpu, was performed on unnormalized data from three independent experiments using GraphPad Prism (version 7.0c). *, $P < 0.05$; **, $P < 0.01$. Error bars are standard deviations. (B) Downregulation of surface BST-2 by wild-type Vpu and Vpu mutants was analyzed by staining the cells with Alexa Fluor 647-conjugated anti-BST-2 antibody, followed by permeabilization and staining with FITC-anti-p24. Cells were analyzed by flow cytometry using a BD Accuri C6 instrument, and the MFI for the AF647 channel was calculated after gating on live $p24^+$ cells using FlowJo software. The values for all the mutants from two independent experiments were normalized to those for ΔVpu and plotted using GraphPad Prism (version 7.0c). Error bars are standard deviations. (C) The 2-color plots from a representative experiment show BST-2 expression (*y* axis) versus intracellular p24 expression (*x* axis). (D) Immunoblot analysis of transfected cells to analyze the expression levels of the Vpu mutants from a representative of three independent experiments. The star indicates a nonspecific band.

QC406.70M.ENV.F3 (GenBank accession number FJ866133) (55, 56), referred to here as C-133. A sequence alignment of the C-133 Vpu compared to MJ4 is shown in Fig. 5A. We evaluated its activity and that of its β-TrCP-binding serine and C-terminal leucine mutants compared to that of the MJ4 Vpu. Figure 5B shows that the ability of C-133 Vpu to enhance virion release is similar to that of MJ4 Vpu, as is its ability to downregulate BST-2 from the cell surface (Fig. 5C) and its expression level (Fig. 5D). As with MJ4 Vpu, mutation of the β-TrCP-binding serines 58 and 62 to asparagines abrogated the downregulation of BST-2 from the cell surface (Fig. 5C) but only partially impaired virion release (Fig. 5B). Conversely, and similar to MJ4 Vpu, mutation of L80 and L81 (LL/AA) in C-133 Vpu did not affect the downregulation of BST-2 from the cell surface (Fig. 5C) but slightly impaired virion release (Fig. 5B). Mutation of both the serines and leucines together (C-133 S58,62N+LL/AA) completely eliminated the ability

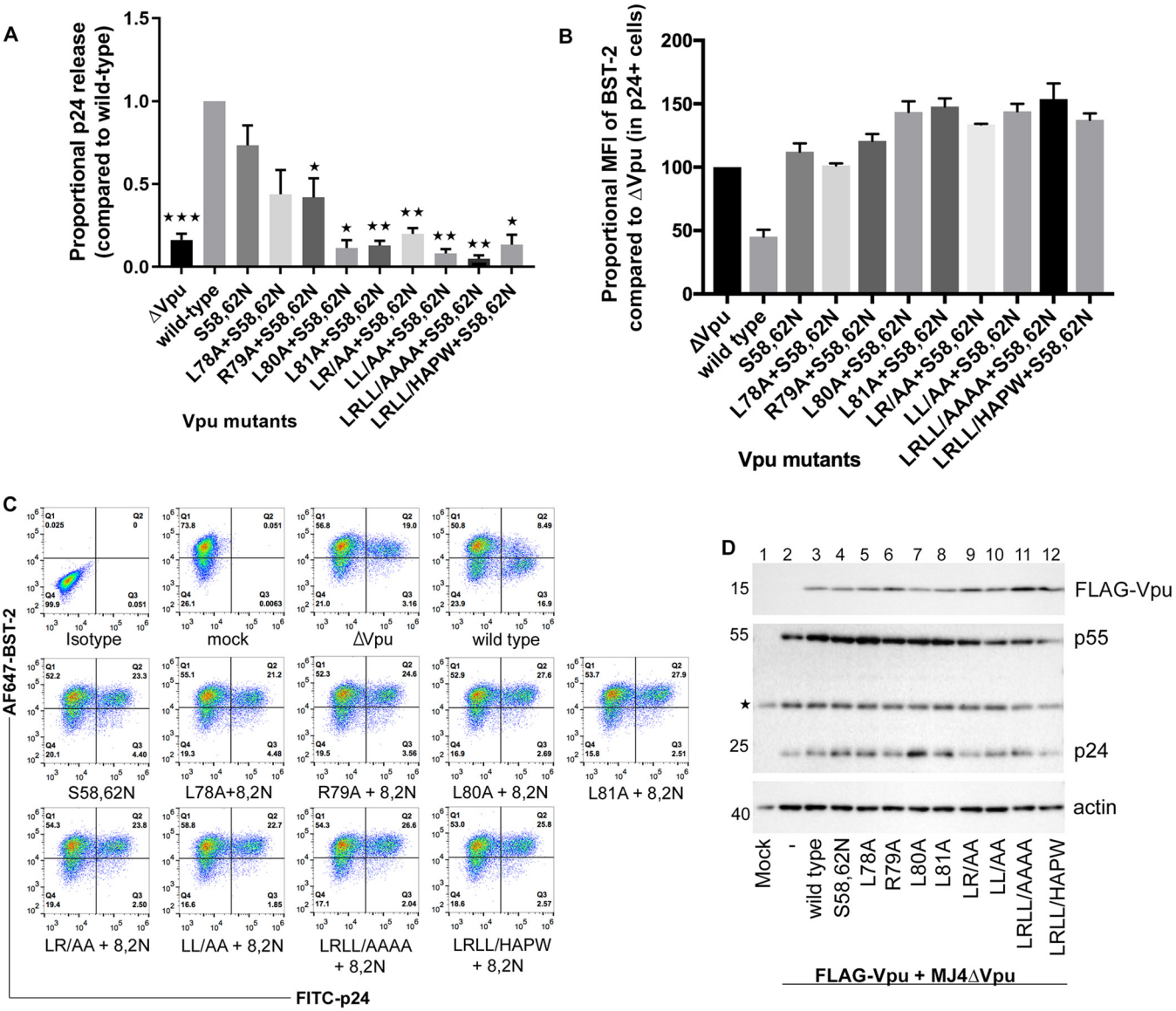

FIG 4 Characterization of C-terminal mutants of Vpu in combination with β-TrCP binding site mutations S58N/S62N. (A) Vpu mutants were analyzed for their ability to enhance virion release as described for Fig. 3. Ratio paired *t* test, compared to data for mutant Vpu-S58,62N, was performed on unnormalized data from three independent experiments (of duplicates) using GraphPad Prism (version 7.0c). *, $P < 0.05$; **, $P < 0.01$; ***, $P < 0.001$. Error bars are standard deviations. (B) Downregulation of surface BST-2 by the Vpu mutants was analyzed as described for Fig. 3 from two independent experiments. The values for all the mutants were normalized to data for ΔVpu. Error bars are standard deviations. (C) The 2-color plots from a representative experiment show BST-2 expression (*y* axis) versus intracellular p24 expression (*x* axis). (D) Immunoblot analysis of transfected cells to analyze the expression levels of the Vpu mutants. A star indicates a nonspecific band.

of Vpu to antagonize BST-2, resulting in virion release levels similar to that of virus lacking *vpu* (ΔVpu).

Mutations within the C terminus do not alter the subcellular localization of clade C Vpu, but they impair the ability of Vpu to displace BST-2 from Gag in the plane of the plasma membrane. Whereas clade B Vpu is primarily present in the endoplasmic reticulum and Golgi network, studies of a different clade C Vpu fused to enhanced green fluorescent protein found that it is also evident on the plasma membrane (57, 58). To establish that the above-described mutations do not cause Vpu to localize aberrantly, we examined transfected cells using immunofluorescence microscopy. HeLa P4-R5 cells were transfected with pMJ4ΔVpu, either alone or along with various Vpu expression constructs. The next day, the cells were stained for BST-2 (red), Vpu as FLAG (blue), and Gag p24 (green). Z-series were collected and projection images

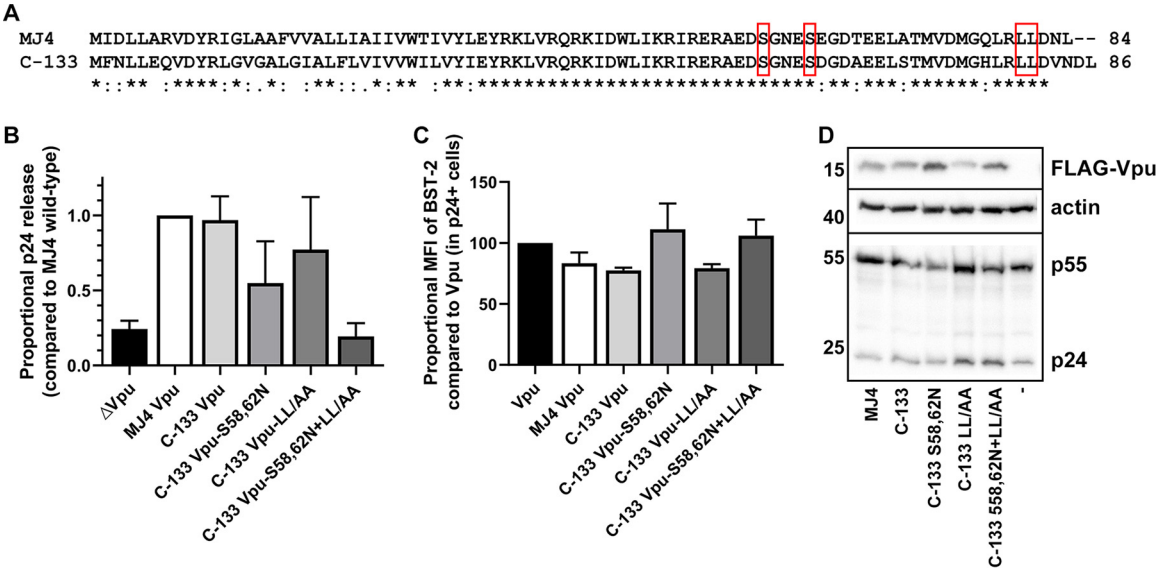

FIG 5 Characterization of a primary clade C Vpu and its phosphoserine and C-terminal dileucine mutants. (A) The sequence alignment of MJ4 Vpu compared with the C-133 Vpu cloned from a primary clade C virus isolated from early infection was generated using Clustal-Omega (EMBL) software. The β-TrCP-binding phosphoserines and dileucines mutated for these experiments are boxed in red. (B) The indicated Vpu mutants were analyzed for their ability to enhance virion release as described for Fig. 3. The data shown are from four independent experiments done in triplicate. Error bars are standard deviations. (C) Downregulation of surface BST-2 by the Vpu mutants was analyzed as described for Fig. 3 for four independent experiments. The values for all the mutants were normalized to those for ΔVpu. Error bars are standard deviations. (D) Immunoblots representative of four independent experiments were performed as described for Fig. 3D to analyze the expression of the Vpu mutants.

were created; representative fields are shown in Fig. 6. All the Vpu mutants are similarly expressed, with typical juxtanuclear concentrations (presumably in the Golgi and *trans*-Golgi network) as well as localization to the plasma membrane, with substantial overlap between BST-2 and Vpu (purple in the merged panels on the right).

We next tested the hypotheses that clade C Vpu displaces BST-2 away from virion assembly sites and that L80 and L81 contribute to this activity. To do this, we measured the colocalization of BST-2 with Gag p24 in the plane of the plasma membrane. The displacement effect is independent of the phosphoserines in clade B Vpu, and in their absence BST-2 is not downregulated from the cell surface or degraded (which would confound the colocalization measurements), so we studied the role of the C-terminal leucines in the context of the S58,62N substitution (47, 50). HeLa P4-R5 cells were transfected with pMJ4ΔVpu, either with empty vector or together with the Vpu expression plasmids. The next day, the cells were stained for BST-2, Gag p24, and Vpu (FLAG). To capture the cell surface in a reproducible manner, Z-series of images were collected along and just above the cover glass, images were processed by a deconvolution algorithm, and the single image plane adjacent to the cover glass was analyzed. Figure 7A shows representative single-plane images of the bottom surface of the cells. Colocalization of BST-2 and Gag (yellow in the fourth column of images, Gag+BST2) appeared to be less when Vpu-S58,S62N was expressed than in cells without Vpu (MJ4ΔVpu alone). This effect of Vpu-S58,62N was lost when either L80 or L81 was replaced with alanine. To quantify these effects, we analyzed multiple single cells for each condition (see dot plots of individual cells in Fig. 7B to D). Each cell was masked completely in the image plane adjacent to the cover glass, and the intensity of Vpu as well as Pearson correlation coefficients between BST-2 and Gag, and between BST-2 and Vpu, were calculated using SlideBook software (version 4.1; Intelligent Imaging Innovations, Denver, CO). Because the expression of Vpu among individual cells was variable, we included only those cells with Vpu intensities between 200 and 300 arbitrary units (Fig. 7C) for subsequent analyses of BST-2/Vpu (Fig. 7B) and of BST-2/Gag (Fig. 7D) colocalization. In these data, a value of +1 indicates perfect correlation, 0 indicates no

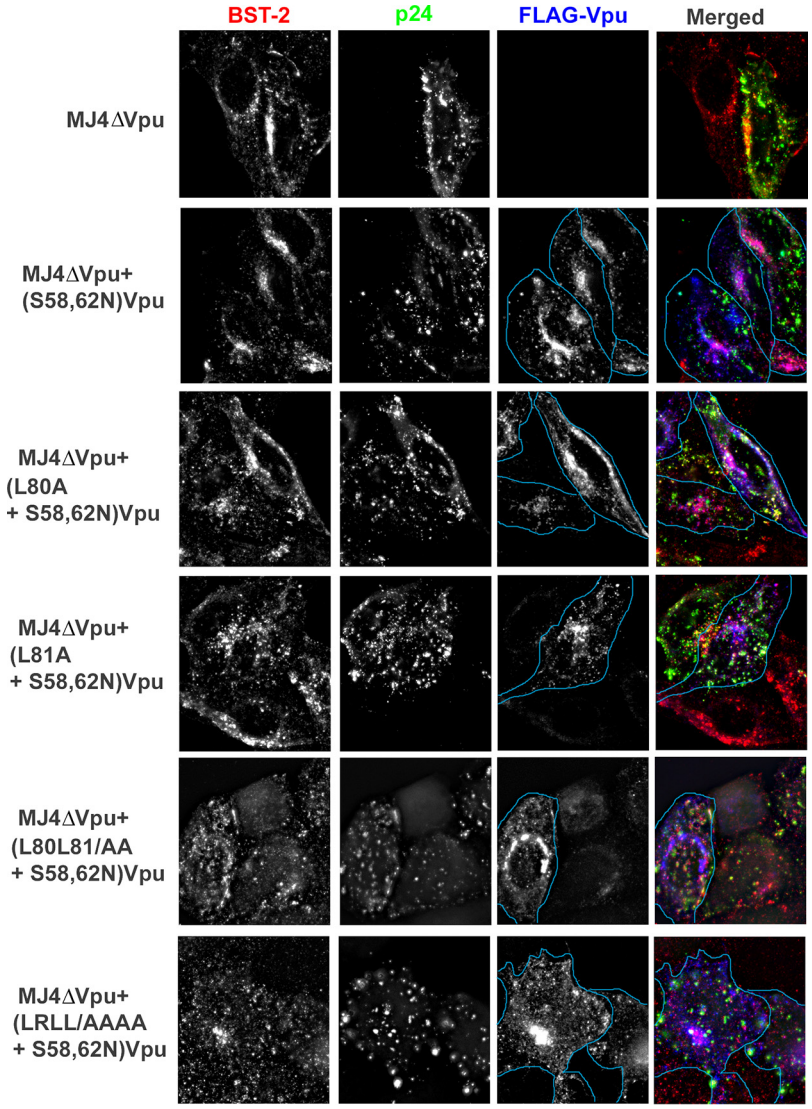

FIG 6 Mutations in the C terminus of Vpu do not affect subcellular localization. HeLa P4-R5 cells were transfected to express MJ4ΔVpu alone or together with the indicated Vpu-S58,62N-FLAG-tagged mutants. The next day, cells were fixed and permeabilized and then stained for BST-2 (red), blocked with mouse serum, and lastly stained for Gag p24 (green) and FLAG (Vpu; blue). The slides were imaged using a wide-field fluorescence microscope (Olympus) and analyzed using SlideBook software (version 4.1; Intelligent Imaging Innovations, Denver, CO). For each field, a series of images along the z-stack was collected and deconvolved using a no-neighbor method, and a projection image was created. Images were assembled using Photoshop (Adobe) software. Vpu-expressing cells were outlined manually.

correlation, and −1 indicates a negative correlation. All the Vpu proteins colocalized similarly with BST-2 (Fig. 7B). In the absence of Vpu, BST-2 and Gag colocalized to a moderate extent, but this colocalization was substantially and significantly decreased when the β-TrCP binding mutant S58,62N was expressed (Fig. 7D). These data represent the BST-2/Gag displacement effect, which is independent of the Vpu phosphoserines. When either the L80A or L81A substitution was added to the S58,62N mutant (Fig. 7D, L80A+S58,62N and L81A+S58,62N), the displacement effect was largely lost, and the colocalization of BST-2 and Gag approached that of the no-Vpu condition (MJ4ΔVpu alone). Taken together, these data suggest that leucines L80 and L81 in clade C Vpu are functionally analogous to W76 in clade B Vpu: they support the displacement of BST-2 from Gag along the plasma membrane and, in doing so, contribute to optimal virion release.

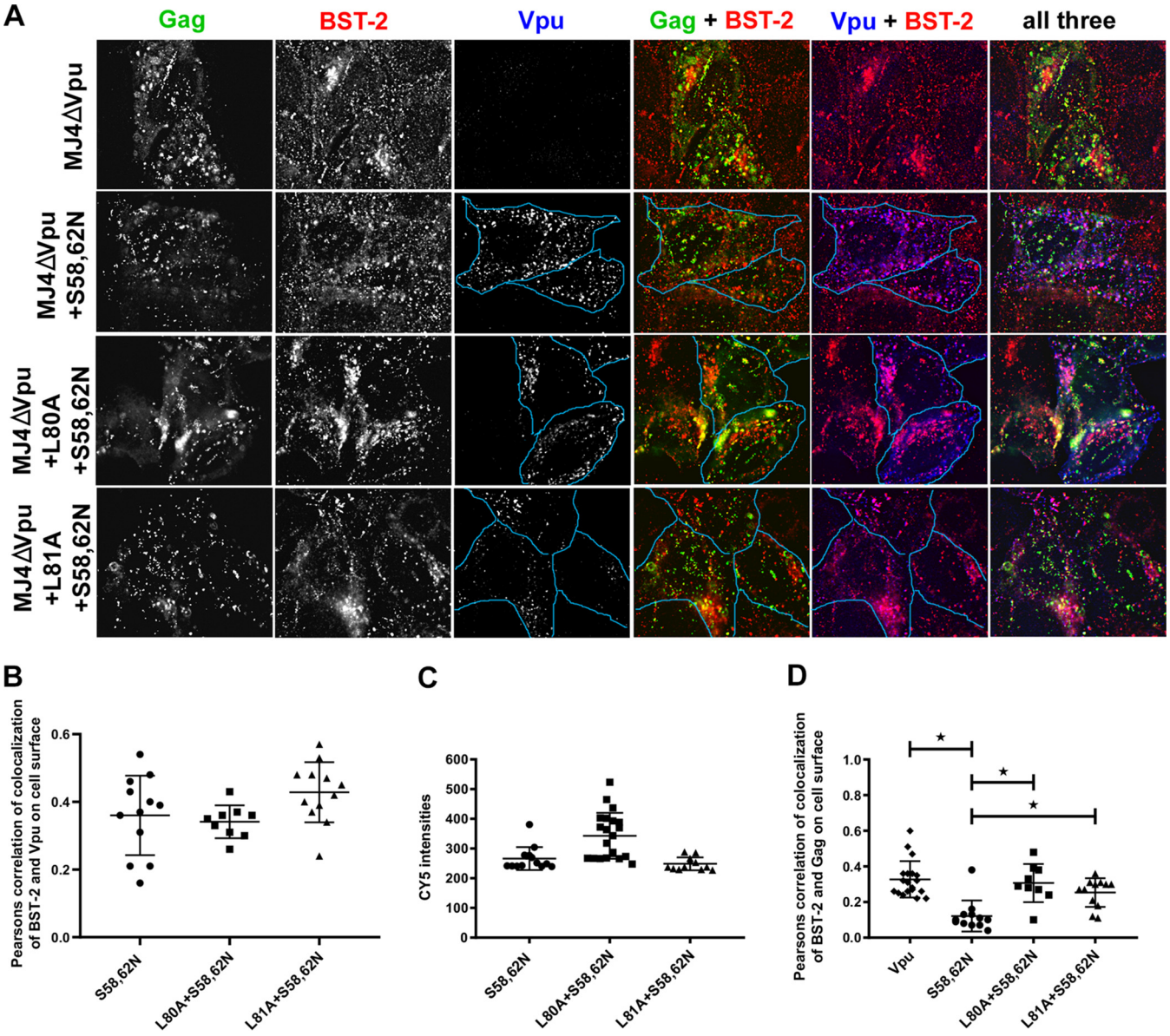

FIG 7 L80 and L81 contribute to the displacement of BST-2 from virion assembly sites. (A) HeLa P4-R5 cells were transfected to express MJ4ΔVpu alone or together with the indicated Vpu-S58,62N-FLAG-tagged mutants. The next day, the cells were fixed and permeabilized and then stained for BST-2 (red), blocked with mouse serum, and lastly stained for Gag p24 (green) and FLAG (Vpu; blue). The slides were imaged using a wide-field fluorescence microscope (Olympus) and analyzed using SlideBook software (version 4.1; Intelligent Imaging Innovations, Denver, CO). For each field, a series of images along the z-stack was collected and deconvolved using a constrained-iterative method, and the section closest to the cover glass was chosen for analysis. Shown here are representative images of such sections assembled using Photoshop (Adobe) software. Vpu-expressing cells were outlined manually. (B) Dot plot showing the quantitated colocalization of Vpu with BST-2; each symbol represents the Pearson correlation coefficient for a single cell. Error bars are standard deviations. (C) Dot plot depicting the expression levels (Cy5 intensity measurements) of Vpu, where each dot represents a single cell. Error bars are standard deviations. (D) Dot plot showing the colocalization of Gag and BST-2 at the cell surface. Each dot represents the Pearson correlation coefficient for BST-2 with Gag, calculated for individual cells. *, $P < 0.001$. Error bars are standard deviations. For panels B and D (except ΔVpu), only those cells with a Vpu (Cy5) intensity between 200 and 300 were analyzed.

Addition of a clathrin binding sequence to the C terminus of Vpu partially rescues virion release activity of the phosphoserine and dileucine combination mutant. We hypothesized that $_{80}LL_{81}$ is part of a clathrin-binding motif, like LΦpΦ(−), where Φ is a bulky hydrophobic residue, p is a polar residue, and (−) is an acidic residue (59). To test this hypothesis, we adopted the strategy employed by Kueck et al. (41) and appended a clathrin box (CB) sequence from the HRS protein to our phosphoserine and C-terminal dileucine mutants of MJ4 Vpu, and then we asked whether this rescued their ability to antagonize BST-2 (Fig. 8). To assess specificity, we also appended a nonfunc-

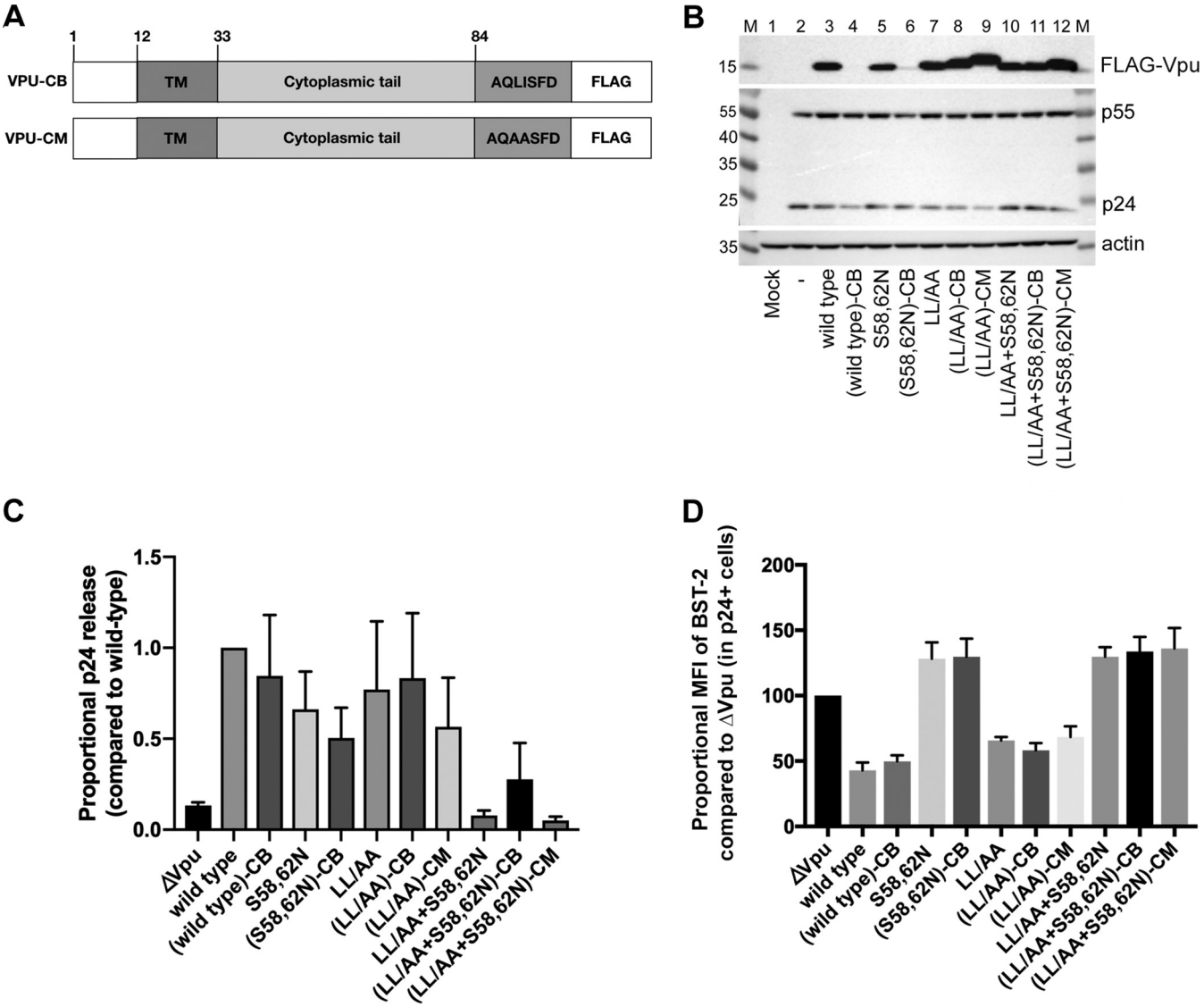

FIG 8 Clathrin box sequence partially rescues the virion release activity of a Vpu phosphoserine and C-terminal leucine combination mutant. (A) Schematic diagram of the clathrin box Vpu constructs. The CM sequence contains alanine substitutions of the LI residues in the CB sequence essential for binding to clathrin. (B) HeLa P4-R5 cells were transfected with MJ4ΔVpu in the absence or presence of the indicated Vpu-CB or Vpu-CM constructs. After 24 h, the cells were harvested and immunoblotted for the expression of Vpu (FLAG). (C) Vpu mutants were analyzed for their ability to enhance virion release as described for Fig. 3 The data shown are from three independent experiments performed in duplicate. Error bars are standard deviations. (D) Downregulation of surface BST-2 by the Vpu mutants was analyzed as described for Fig. 3 for two independent experiments. The values for all the mutants were normalized to those for ΔVpu. Error bars are standard deviations.

tional version of the clathrin box sequence (CM; amino acid sequence shown in Fig. 8A) to the Vpu proteins. HeLa P4-R5 cells were transfected with these Vpu constructs and *vpu*-negative provirus (pMJ4ΔVpu) as before. Cells were harvested for immunostaining and analysis by flow cytometry, lysates were collected for immunoblotting, and supernates were harvested to assess the quantities of released virions. The representative immunoblots in Fig. 8B show that fusion of the CB sequence to wild-type and S58,62N mutant Vpus dramatically decreased their expression (compare lane 3 with 4 and lane 5 with 6 in the FLAG-Vpu row). In contrast, the LL/AA-CB and (LL/AA+S58,62N)-CB proteins, as well as the corresponding -CM versions, were all well expressed, allowing a comparison of their relative activities. The enhancement of virion release by the Vpu-LL/AA mutant was not significantly affected by either the CB or CM sequences (Fig. 8C). However, the CB sequence substantially increased virion release when appended to Vpu-LL/AA+S58,62N. This increase did

not approach the levels of wild-type Vpu or even the LL/AA or S58,62N individual motif mutants, but it was specific to the CB and not the CM sequence. Cell surface downregulation of BST-2 was not rescued by the addition of the CB sequence to any mutant (Fig. 8D). Although appending the CB sequence to the Vpu-S58,62N mutant failed to rescue either BST-2 downregulation or virion release, the strikingly low expression of Vpu-S58,62N-CB relative to that of Vpu-S58,62N rendered this comparison problematic (Fig. 8B, compare lanes 5 and 6). Taken together, these data suggest that a clathrin-binding sequence can partially provide the activity naturally carried by L80 and L81 in the clade C Vpu C terminus with respect to enhancing virion release, but whether this is due to clathrin binding or simply the hydrophobic property of the sequence is unclear.

DISCUSSION

The accessory proteins of HIV-1 contribute to the establishment and spread of infection by counteracting various innate and adaptive immune responses. In the case of Vpu, the antagonism of BST-2 not only facilitates the dissemination of cell-free virions but also decreases the amount of virion-associated Env glycoprotein on the surface of the infected cell, thereby reducing the effectiveness of immune clearance mediated by antibody-dependent cellular cytotoxicity (ADCC) (60–62). Although a relatively small protein, Vpu is packed with a variety of motifs that enable the coopting of seemingly diverse host cellular machinery, including short peptide sequences that bind to the β-TrCP-containing cullin1-based E3 ubiquitin ligase complex and to clathrin adaptor protein complexes. Together, these interactions enable Vpu to degrade and mistraffic targets such as BST-2.

A unified model of Vpu activity has been elusive; instead, several mechanisms appear to contribute, one of which is the apparent ability of Vpu to displace BST-2 from Gag in the plane of the plasma membrane. This displacement activity presumably provides nascent virions a means to escape entrapment by BST-2, even when the total amount of BST-2 on the cell surface is not decreased. To our knowledge, the displacement effect so far has been shown exclusively with clade B Vpu proteins. Moreover, it depends on a residue, W76, which is not present in clades such as A and C. Here, we show that the C-terminal region of clade C Vpu contains a conserved LL motif that provides an activity analogous to that of W76 in clade B viruses: it contributes to enhancing virion release in conjunction with the hinge region phosphoserines that have a dual role in recruiting the ubiquitin-ligase and clathrin adaptor complexes, and it supports the displacement of BST-2 from Gag in the plane of the plasma membrane.

What is the mechanism by which the LL motif functions? Given the hydrophobic nature of the leucines and their similar position to W76 in clade B Vpu, they might, like W76, provide a membrane-anchoring activity through which the Vpu C terminus is fixed to the lipid bilayer (50). Alternatively, we considered that the sequence near the C-terminal end of clade C Vpu is reminiscent of the clathrin-binding motif LΦpΦ(−) (59). Specifically, the sequence $_{78}$LR**LLDVND**$_{85}$, in which the boldfaced residues are an imperfect but near match to the foregoing clathrin-binding sequence, led us to speculate that L80 and L81 support clathrin-binding activity. If so, then the C-terminal Vpu mutants might be unable to direct BST-2 to clathrin coats. This might underlie the mechanism of the displacement effect, if that effect involves the recruitment of BST-2 to clathrin-coated domains of the plasma membrane. However, when we appended the HRS clathrin box (CB) sequence to the C-terminal end of our Vpu mutants, the effects were inconclusive. Unexpected negative effects on protein expression prevented confirming that the CB sequence rescued the S58,62N mutation, as predicted by previous work using the clade B Vpu from NL4-3 (41). The basis for these negative effects of the CB sequence on protein expression at steady state are unclear, and remarkably they occurred only when the C-terminal LL sequence was intact. Moreover, despite its markedly reduced expression, the wild-type clade C Vpu appended with the CB sequence paradoxically retained the ability to enhance virion release and to downregulate BST-2. One possibility is that the CB and LL sequences together yield an affinity

for clathrin coats that causes Vpu to be degraded in lysosomes together with its targets. Regarding the hypothesis that L80 and L81 are part of a clathrin-binding sequence, the virion release phenotype of the Vpu-LL/AA+S58,62N mutant was partially rescued by the CB sequence (and not by a related mutant of that sequence predicted not to bind clathrin), but this rescue was not to the level of Vpu-S58,56N, as it should have been if the CB sequence had substituted fully for L80 and L81.

The notion that clathrin coats are involved in the displacement effect is not without precedent: the ExxxLV clathrin adaptor protein binding motif in helix 2 of the cytoplasmic domain of clade B Vpu was reported to support the displacement effect (47), and the effect was reportedly inhibited by expression of a dominant-negative version of the clathrin assembly protein AP180 and by knockdown of the AP-1 clathrin adaptor via short interfering RNA (63). A caveat to the latter study is that the hinge phosphoserines were reported as required for the displacement effect, whereas we and others have found them dispensable and, by design, here have studied the effect in their absence (47, 50, 63). Could W76 of clade B Vpu also be part of a clathrin-binding sequence? This is plausible, since PWDLW is a clathrin-binding sequence and is reminiscent of the $_{75}$PWDID$_{79}$ clade B sequence of which W76 is a part (59).

Does the LL motif in clade C support other activities that have been associated with W76 in clade B Vpu, such as the downregulation of CD1d? The $_{74}$APW$_{76}$ sequence of clade B Vpu is reportedly required for the downregulation of CD1d (64). Clade C Vpu proteins are relatively poorly active in this regard, but if those that are active require the $_{78}$LRLL$_{81}$ or $_{80}$LL$_{81}$ sequence, then the functional equivalency of these regions in clade B and C Vpu proteins would be further supported.

A final question is the following: why have the different clades of HIV-1 evolved to encode the BST-2 displacement activity differently? While the answer must be speculative, we note that the W76G polymorphism in clade B Vpu occurs in a predicted epitope for cytotoxic T lymphocytes (CTLs) and is probably a CTL escape mutation. In our previous study of pairs of Vpu proteins derived from patients during the acute and chronic stages of infection, the W76G polymorphism developed over time (49). Apparently, the fitness cost of losing the displacement effect was less than that of remaining susceptible to CTL activity. Conceivably, the clade C LL sequence might support the displacement effect while providing a relatively poor target for CTLs.

In summary, we show that the C-terminal region of clade C Vpu harbors a dileucine motif that, in conjunction with phosphoserines in the protein's hinge region, plays an important role in enhancing virion release. This sequence appears to function analogously to W76 in clade B Vpu to support the displacement of BST-2 from virion assembly sites. The mechanism of this effect and how it is supported by these different sequences remains to be determined.

MATERIALS AND METHODS

Plasmids, cells, and reagents. The proviral plasmid pMJ4 was obtained through the NIH AIDS Reagent Program, NIAID, NIH; HIV-1 MJ4 was from Thumbi Ndung'u, Boris Renjifo, and Max Essex (54). The *vpu*-negative pMJ4ΔVpu was constructed by inserting termination codons in place of Vpu residues 10 and 13 using the QuikChange XL site-directed mutagenesis kit (Agilent). The *vpu* mutant clone pMJ4-Vpu-S58,62N was constructed using QuikChange. For the Rev-dependent FLAG-tagged MJ4-Vpu expression construct, the *vpu* coding region from pMJ4 was amplified by PCR with primers designed to introduce a C-terminal FLAG tag, gel purified using a QIAquick gel extraction kit (Qiagen), and then cloned into the pcDNA-RRE expression vector (described in reference 49) after digestion of the purified PCR products and backbone with NheI and XhoI (NEB). Expression plasmids encoding Vpu-L78A, Vpu-R79A, Vpu-L80A, Vpu-L81A, Vpu L78A,R79A (LR/AA), Vpu-L80A,L81A (LL/AA), Vpu-L78A,R79A,L80A,L81A (LRLL/AAAA), and Vpu-L78H,R79A,L80P,L81W (LRLL/HAPW) with a C-terminal FLAG tag were made by QuikChange site-directed mutagenesis (Agilent) of the MJ4-Vpu-FLAG expression construct. Expression plasmids encoding Vpu-S58,62N+L78A, Vpu-S58,62N+R79A, Vpu-S58,62N+L80A, Vpu-S58,62N+L81A, Vpu-S58,62N+L78A,R79A (LR/AA+S58,62N), Vpu-S58,62N+L80A,L81A (LL/AA+S58,62N), Vpu-S58,62N+L78A,R79A,L80A,L81A (LRLL/AAAA+S58,62N), and Vpu-S58,62N+L78H,R79A,L80P,L81W (LRLL/HAPW+S58,62N) with a C-terminal FLAG tag were made by site-directed mutagenesis of the MJ4-Vpu S58,62N-FLAG expression construct using QuikChange. The C-133 Vpu construct and mutants were cloned similarly from the following reagent, which was obtained through the NIH AIDS Reagent Program, Division of AIDS, NIAID, NIH: clone QC406.70M.ENV.F3 (GenBank accession number FJ866133; catalog number 11910) from Julie Overbaugh (55, 56). The clathrin box (CB)

sequence (AQLISFD) from HRS was inserted before the C-terminal FLAG tag using site-directed mutagenesis to create wtVpu-CB-FLAG, (S58,62N)-CB-FLAG, (LL/AA)-CB-FLAG, and (LL/AA+S58,62N)-CB-FLAG. The mutated sequence (AQAASFD) of the HRS CB (referred to as CM) was also inserted before the C-terminal FLAG tag using site-directed mutagenesis to create (LL/AA)-CM-FLAG and (LL/AA+S58,62N)-CM-FLAG. All sequences were verified by Sanger sequencing (GENEWIZ).

Transfections. One day prior to transfection, HeLa P4-R5 cells were seeded in 12-well plates in Dulbecco's modified Eagle's medium (DMEM) supplemented with 10% fetal bovine serum and penicillin-streptomycin at a density of 180,000 cells per well. The next day they were transfected with either 600 ng of proviral plasmid pMJ4ΔVpu plus 500 ng of empty vector [pcDNA3.1(−)] or 600 ng of proviral plasmid pMJ4ΔVpu plus 500 ng of Rev-dependent Vpu-FLAG expression plasmid in duplicate using Lipofectamine 2000 (Thermo Fisher Scientific). Cells and supernates were collected the next day and were used for flow cytometry, p24 ELISA, and immunoblot analysis.

Virion release assays. Supernates from HeLa P4-R5 cells transfected with the proviral plasmid alone or with Vpu expression constructs were collected and pelleted through 20% sucrose cushions. Supernatant Gag was quantitated by p24 ELISA (Perkin-Elmer).

Immunoblots. Transfected HeLa P4-R5 cells were collected and lysed in 1× Laemmli sample buffer. The lysates were run on 10% polyacrylamide gels, blotted onto polyvinylidene difluoride membranes, and probed for actin (mouse anti-β-actin, AC-74; Sigma), FLAG (mouse anti-FLAG M2; Sigma), and Gag (mouse anti-HIV-1 gag, MAB880-A; EMD Millipore), followed by goat anti-mouse-horseradish peroxidase conjugate (Bio-Rad). The blots were developed using enhanced chemiluminescence substrate (Bio-Rad) and imaged using the ChemiDoc MP system (Bio-Rad).

Flow cytometry. Transfected HeLa P4-R5 cells were stained with Alexa Fluor 647-conjugated mouse anti-human CD317 (BST-2, RS38E; BioLegend) or its isotope control, Alexa Fluor 647-conjugated mouse IgG1k, according to the manufacturer's instructions. Cells were washed and then fixed and permeabilized using the BD Cytofix/Cytoperm kit according to the manufacturer's instructions. The cells were then stained with FITC-conjugated anti-HIV-1 p24 antibody (KC57; Beckman Coulter) and analyzed using a BD Accuri C6 flow cytometer and FlowJo software (TreeStar). Cell surface expression of BST-2 was quantitated after gating on the live p24-positive population.

Immunofluorescence microscopy. Immunofluorescence microscopy was performed as described previously (50), with some modifications. Briefly, HeLa P4-R5 cells were seeded at 100,000 cells per well on glass coverslips in a 24-well plate a day before transfection. Cells were transfected with 450 ng of the proviral plasmid pMJ4ΔVpu and 350 ng of FLAG-tagged Vpu expression constructs using Lipofectamine 2000 (Thermo Fisher). Four hours later, the culture medium was changed to complete DMEM, supplemented with 30 ng/ml of human alpha interferon A/D (Sigma) to increase BST-2 expression for improved detection, and left overnight. The next day, the cell culture medium was aspirated and cells were washed twice with phosphate-buffered saline (PBS). Cells were fixed using 3% paraformaldehyde for 15 min at 4°C. After two washes with PBS, cells were permeabilized using 0.2% NP-40 for 7 min at 4°C. Again, the cells were washed twice and then were blocked with 5% donkey serum and 3% bovine serum albumin in PBS for 30 min at 4°C. After a single PBS wash, cells were stained with a 1:300 dilution of mouse anti-BST-2/HM1.24/CD317 antibody (Chugai Pharmaceutical Co., Kanagawa, Japan) for 30 min at 4°C. After 4 washes with PBS, cells were stained with a 1:500 dilution of Rhodamine Red-X-conjugated donkey anti-mouse antibody (Jackson ImmunoResearch) for 30 min at 4°C. After 5 washes with PBS, cells were blocked with 5% mouse serum for 30 min at 4°C. After a PBS wash, cells were stained with FITC-conjugated mouse anti-HIV-1 p24 antibody (KC57; Beckman Coulter), diluted 1:150, and AF647-conjugated rabbit anti-FLAG, diluted 1:200 (Cell Signaling), for 30 min at 4°C. Cells were then washed 5 times with PBS, and coverslips were mounted on glass slides using Pierce gold antifade reagent (Pierce) and were left to dry overnight before imaging. Images were acquired using a fluorescence microscope (Olympus) and SlideBook (version 4.1; Intelligent Imaging Innovations, Denver, CO). For each field, series of z-stacks closest to the cover glass were collected, images were deconvolved using the SlideBook software Constrained Iterative (CI) method, and a representative single-image plane was chosen and assembled using Photoshop software (Adobe).

For the quantitation of colocalization, the images were deconvolved using the CI method and a single plane closest to the cover glass was chosen. A mask was made on the entire cell, and the Pearson correlation coefficient between BST-2 and Gag and between BST-2 and Vpu was calculated for the whole cell. For each cell analyzed, Vpu intensity was also calculated in all samples where Vpu expression constructs were transfected along with the provirus. The values of Vpu intensity were plotted using GraphPad Prism software. A midrange set of values of 200 to 300 was selected as an acceptable expression level of Vpu. The Pearson correlation coefficients of BST-2 and Gag were plotted and analyzed for only those cells which had a Vpu expression intensity between 200 and 300 arbitrary units.

ACKNOWLEDGMENTS

This work was funded by R21AI114397 and R37AI081668 to J.G. M.K.L. was supported by K08AI112394. We are thankful to The James B. Pendleton Charitable Trust for equipment and support, Marissa Suarez for performing the p24 ELISA assays, and the members of the Guatelli laboratory for helpful discussions. S.S., J.G., and M.K.L. designed the experiments; S.S. and M.K.L. performed the experiments; M.J., A.B., K.W., and M.K.L. performed the cloning of the constructs; S.S., J.G., and M.K.L. analyzed the data and wrote the manuscript.

REFERENCES

1. Sheehy AM, Gaddis NC, Choi JD, Malim MH. 2002. Isolation of a human gene that inhibits HIV-1 infection and is suppressed by the viral Vif protein. Nature 418:646–650. https://doi.org/10.1038/nature00939.
2. Stremlau M, Owens CM, Perron MJ, Kiessling M, Autissier P, Sodroski J. 2004. The cytoplasmic body component TRIM5alpha restricts HIV-1 infection in Old World monkeys. Nature 427:848–853. https://doi.org/10.1038/nature02343.
3. Sayah DM, Sokolskaja E, Berthoux L, Luban J. 2004. Cyclophilin A retrotransposition into TRIM5 explains owl monkey resistance to HIV-1. Nature 430:569–573. https://doi.org/10.1038/nature02777.
4. Laguette N, Sobhian B, Casartelli N, Ringeard M, Chable-Bessia C, Segeral E, Yatim A, Emiliani S, Schwartz O, Benkirane M. 2011. SAMHD1 is the dendritic- and myeloid-cell-specific HIV-1 restriction factor counteracted by Vpx. Nature 474:654–657. https://doi.org/10.1038/nature10117.
5. Hrecka K, Hao C, Gierszewska M, Swanson SK, Kesik-Brodacka M, Srivastava S, Florens L, Washburn MP, Skowronski J. 2011. Vpx relieves inhibition of HIV-1 infection of macrophages mediated by the SAMHD1 protein. Nature 474:658–661. https://doi.org/10.1038/nature10195.
6. Berger A, Sommer AFR, Zwarg J, Hamdorf M, Welzel K, Esly N, Panitz S, Reuter A, Ramos I, Jatiani A, Mulder LCF, Fernandez-Sesma A, Rutsch F, Simon V, König R, Flory E. 2011. SAMHD1-deficient CD14+ cells from individuals with Aicardi-Goutieres syndrome are highly susceptible to HIV-1 infection. PLoS Pathog 7:e1002425. https://doi.org/10.1371/journal.ppat.1002425.
7. Baldauf HM, Pan X, Erikson E, Schmidt S, Daddacha W, Burggraf M, Schenkova K, Ambiel I, Wabnitz G, Gramberg T, Panitz S, Flory E, Landau NR, Sertel S, Rutsch F, Lasitschka F, Kim B, Konig R, Fackler OT, Keppler OT. 2012. SAMHD1 restricts HIV-1 infection in resting CD4(+) T cells. Nat Med 18:1682–1687. https://doi.org/10.1038/nm.2964.
8. Descours B, Cribier A, Chable-Bessia C, Ayinde D, Rice G, Crow Y, Yatim A, Schwartz O, Laguette N, Benkirane M. 2012. SAMHD1 restricts HIV-1 reverse transcription in quiescent CD4(+) T-cells. Retrovirology 9:87. https://doi.org/10.1186/1742-4690-9-87.
9. Rosa A, Chande A, Ziglio S, De Sanctis V, Bertorelli R, Goh SL, McCauley SM, Nowosielska A, Antonarakis SE, Luban J, Santoni FA, Pizzato M. 2015. HIV-1 Nef promotes infection by excluding SERINC5 from virion incorporation. Nature 526:212–217. https://doi.org/10.1038/nature15399.
10. Usami Y, Wu Y, Gottlinger HG. 2015. SERINC3 and SERINC5 restrict HIV-1 infectivity and are counteracted by Nef. Nature 526:218–223. https://doi.org/10.1038/nature15400.
11. Neil SJ, Zang T, Bieniasz PD. 2008. Tetherin inhibits retrovirus release and is antagonized by HIV-1 Vpu. Nature 451:425–430. https://doi.org/10.1038/nature06553.
12. Van Damme N, Goff D, Katsura C, Jorgenson RL, Mitchell R, Johnson MC, Stephens EB, Guatelli J. 2008. The interferon-induced protein BST-2 restricts HIV-1 release and is downregulated from the cell surface by the viral Vpu protein. Cell Host Microbe 3:245–252. https://doi.org/10.1016/j.chom.2008.03.001.
13. Kupzig S, Korolchuk V, Rollason R, Sugden A, Wilde A, Banting G. 2003. Bst-2/HM1.24 is a raft-associated apical membrane protein with an unusual topology. Traffic 4:694–709. https://doi.org/10.1034/j.1600-0854.2003.00129.x.
14. Nguyen DH, Hildreth JE. 2000. Evidence for budding of human immunodeficiency virus type 1 selectively from glycolipid-enriched membrane lipid rafts. J Virol 74:3264–3272. https://doi.org/10.1128/JVI.74.7.3264-3272.2000.
15. Jouvenet N, Neil SJ, Zhadina M, Zang T, Kratovac Z, Lee Y, McNatt M, Hatziioannou T, Bieniasz PD. 2009. Broad-spectrum inhibition of retroviral and filoviral particle release by tetherin. J Virol 83:1837–1844. https://doi.org/10.1128/JVI.02211-08.
16. Kaletsky RL, Francica JR, Agrawal-Gamse C, Bates P. 2009. Tetherin-mediated restriction of filovirus budding is antagonized by the Ebola glycoprotein. Proc Natl Acad Sci U S A 106:2886–2891. https://doi.org/10.1073/pnas.0811014106.
17. Mansouri M, Viswanathan K, Douglas JL, Hines J, Gustin J, Moses AV, Fruh K. 2009. Molecular mechanism of BST2/tetherin downregulation by K5/MIR2 of Kaposi's sarcoma-associated herpesvirus. J Virol 83:9672–9681. https://doi.org/10.1128/JVI.00597-09.
18. Sakuma T, Sakurai A, Yasuda J. 2009. Dimerization of tetherin is not essential for its antiviral activity against Lassa and Marburg viruses. PLoS One 4:e6934. https://doi.org/10.1371/journal.pone.0006934.
19. Galao RP, Le Tortorec A, Pickering S, Kueck T, Neil SJ. 2012. Innate sensing of HIV-1 assembly by tetherin induces NFkappaB-dependent proinflammatory responses. Cell Host Microbe 12:633–644. https://doi.org/10.1016/j.chom.2012.10.007.
20. Rizk MG, Basler CF, Guatelli J. 2017. Cooperation of the Ebola virus proteins VP40 and GP1,2 with BST2 to activate NF-kappaB independently of virus-like particle trapping. J Virol 91:e01308-17. doi: 10.1128/JVI.01308-17.
21. Li SX, Barrett BS, Guo K, Kassiotis G, Hasenkrug KJ, Dittmer U, Gibbert K, Santiago ML. 2016. Tetherin/BST-2 promotes dendritic cell activation and function during acute retrovirus infection. Sci Rep 6:20425. https://doi.org/10.1038/srep20425.
22. Hauser H, Lopez LA, Yang SJ, Oldenburg JE, Exline CM, Guatelli JC, Cannon PM. 2011. HIV-1 Vpu and HIV-2 Env counteract BST-2/tetherin by sequestration in a perinuclear compartment. Retrovirology 8:85. https://doi.org/10.1186/1742-4690-8-85.
23. Le Tortorec A, Neil SJ. 2009. Antagonism to and intracellular sequestration of human tetherin by the human immunodeficiency virus type 2 envelope glycoprotein. J Virol 83:11966–11978. https://doi.org/10.1128/JVI.01515-09.
24. Jia B, Serra-Moreno R, Neidermyer W, Rahmberg A, Mackey J, Fofana IB, Johnson WE, Westmoreland S, Evans DT. 2009. Species-specific activity of SIV Nef and HIV-1 Vpu in overcoming restriction by tetherin/BST2. PLoS Pathog 5:e1000429. https://doi.org/10.1371/journal.ppat.1000429.
25. Zhang F, Wilson SJ, Landford WC, Virgen B, Gregory D, Johnson MC, Munch J, Kirchhoff F, Bieniasz PD, Hatziioannou T. 2009. Nef proteins from simian immunodeficiency viruses are tetherin antagonists. Cell Host Microbe 6:54–67. https://doi.org/10.1016/j.chom.2009.05.008.
26. Bartee E, McCormack A, Fruh K. 2006. Quantitative membrane proteomics reveals new cellular targets of viral immune modulators. PLoS Pathog 2:e107. https://doi.org/10.1371/journal.ppat.0020107.
27. Marassi FM, Ma C, Gratkowski H, Straus SK, Strebel K, Oblatt-Montal M, Montal M, Opella SJ. 1999. Correlation of the structural and functional domains in the membrane protein Vpu from HIV-1. Proc Natl Acad Sci U S A 96:14336–14341. https://doi.org/10.1073/pnas.96.25.14336.
28. Park SH, De Angelis AA, Nevzorov AA, Wu CH, Opella SJ. 2006. Three-dimensional structure of the transmembrane domain of Vpu from HIV-1 in aligned phospholipid bicelles. Biophys J 91:3032–3042. https://doi.org/10.1529/biophysj.106.087106.
29. Schubert U, Schneider T, Henklein P, Hoffmann K, Berthold E, Hauser H, Pauli G, Porstmann T. 1992. Human-immunodeficiency-virus-type-1-encoded Vpu protein is phosphorylated by casein kinase II. Eur J Biochem 204:875–883. https://doi.org/10.1111/j.1432-1033.1992.tb16707.x.
30. Schubert U, Henklein P, Boldyreff B, Wingender E, Strebel K, Porstmann T. 1994. The human immunodeficiency virus type 1 encoded Vpu protein is phosphorylated by casein kinase-2 (CK-2) at positions Ser52 and Ser56 within a predicted alpha-helix-turn-alpha-helix-motif. J Mol Biol 236:16–25. https://doi.org/10.1006/jmbi.1994.1114.
31. Schubert U, Strebel K. 1994. Differential activities of the human immunodeficiency virus type 1-encoded Vpu protein are regulated by phosphorylation and occur in different cellular compartments. J Virol 68:2260–2271.
32. Margottin F, Bour SP, Durand H, Selig L, Benichou S, Richard V, Thomas D, Strebel K, Benarous R. 1998. A novel human WD protein, h-beta TrCp, that interacts with HIV-1 Vpu connects CD4 to the ER degradation pathway through an F-box motif. Mol Cell 1:565–574. https://doi.org/10.1016/S1097-2765(00)80056-8.
33. Willey RL, Maldarelli F, Martin MA, Strebel K. 1992. Human immunodeficiency virus type 1 Vpu protein induces rapid degradation of CD4. J Virol 66:7193–7200.
34. Binette J, Dube M, Mercier J, Halawani D, Latterich M, Cohen EA. 2007. Requirements for the selective degradation of CD4 receptor molecules by the human immunodeficiency virus type 1 Vpu protein in the endoplasmic reticulum. Retrovirology 4:75. https://doi.org/10.1186/1742-4690-4-75.
35. Magadan JG, Bonifacino JS. 2012. Transmembrane domain determinants of CD4 downregulation by HIV-1 Vpu. J Virol 86:757–772. https://doi.org/10.1128/JVI.05933-11.
36. Iwabu Y, Fujita H, Kinomoto M, Kaneko K, Ishizaka Y, Tanaka Y, Sata T, Tokunaga K. 2009. HIV-1 accessory protein Vpu internalizes cell-surface BST-2/tetherin through transmembrane interactions leading to lysosomes. J Biol Chem 284:35060–35072. https://doi.org/10.1074/jbc.M109.058305.

37. Douglas JL, Viswanathan K, McCarroll MN, Gustin JK, Fruh K, Moses AV. 2009. Vpu directs the degradation of the human immunodeficiency virus restriction factor BST-2/Tetherin via a β-TrCP-dependent mechanism. J Virol 83:7931–7947. https://doi.org/10.1128/JVI.00242-09.
38. Andrew AJ, Miyagi E, Strebel K. 2011. Differential effects of human immunodeficiency virus type 1 Vpu on the stability of BST-2/tetherin. J Virol 85:2611–2619. https://doi.org/10.1128/JVI.02080-10.
39. Schmidt S, Fritz JV, Bitzegeio J, Fackler OT, Keppler OT. 2011. HIV-1 Vpu blocks recycling and biosynthetic transport of the intrinsic immunity factor CD317/tetherin to overcome the virion release restriction. mBio 2:e00036-11. https://doi.org/10.1128/mBio.00036-11.
40. Dube M, Paquay C, Roy BB, Bego MG, Mercier J, Cohen EA. 2011. HIV-1 Vpu antagonizes BST-2 by interfering mainly with the trafficking of newly synthesized BST-2 to the cell surface. Traffic 12:1714–1729. https://doi.org/10.1111/j.1600-0854.2011.01277.x.
41. Kueck T, Foster TL, Weinelt J, Sumner JC, Pickering S, Neil SJ. 2015. Serine phosphorylation of HIV-1 Vpu and its binding to tetherin regulates interaction with clathrin adaptors. PLoS Pathog 11:e1005141. https://doi.org/10.1371/journal.ppat.1005141.
42. Stoneham CA, Singh R, Jia X, Xiong Y, Guatelli J. 2017. Endocytic activity of HIV-1 Vpu: phosphoserine-dependent interactions with clathrin adaptors. Traffic 18:545–561. https://doi.org/10.1111/tra.12495.
43. Kueck T, Neil SJ. 2012. A cytoplasmic tail determinant in HIV-1 Vpu mediates targeting of tetherin for endosomal degradation and counteracts interferon-induced restriction. PLoS Pathog 8:e1002609. https://doi.org/10.1371/journal.ppat.1002609.
44. Dube M, Roy BB, Guiot-Guillain P, Binette J, Mercier J, Chiasson A, Cohen EA. 2010. Antagonism of tetherin restriction of HIV-1 release by Vpu involves binding and sequestration of the restriction factor in a perinuclear compartment. PLoS Pathog 6:e1000856. https://doi.org/10.1371/journal.ppat.1000856.
45. Jia X, Weber E, Tokarev A, Lewinski M, Rizk M, Suarez M, Guatelli J, Xiong Y. 2014. Structural basis of HIV-1 Vpu-mediated BST2 antagonism via hijacking of the clathrin adaptor protein complex 1. Elife 3:e02362. https://doi.org/10.7554/eLife.02362.
46. Goffinet C, Homann S, Ambiel I, Tibroni N, Rupp D, Keppler OT, Fackler OT. 2010. Antagonism of CD317 restriction of human immunodeficiency virus type 1 (HIV-1) particle release and depletion of CD317 are separable activities of HIV-1 Vpu. J Virol 84:4089–4094. https://doi.org/10.1128/JVI.01549-09.
47. McNatt MW, Zang T, Bieniasz PD. 2013. Vpu binds directly to tetherin and displaces it from nascent virions. PLoS Pathog 9:e1003299. https://doi.org/10.1371/journal.ppat.1003299.
48. Miyagi E, Andrew AJ, Kao S, Strebel K. 2009. Vpu enhances HIV-1 virus release in the absence of Bst-2 cell surface down-modulation and intracellular depletion. Proc Natl Acad Sci U S A 106:2868–2873. https://doi.org/10.1073/pnas.0813223106.
49. Jafari M, Guatelli J, Lewinski MK. 2014. Activities of transmitted/founder and chronic clade B HIV-1 Vpu and a C-terminal polymorphism specifically affecting virion release. J Virol 88:5062–5078. https://doi.org/10.1128/JVI.03472-13.
50. Lewinski MK, Jafari M, Zhang H, Opella SJ, Guatelli J. 2015. Membrane anchoring by a C-terminal tryptophan enables HIV-1 Vpu to displace bone marrow stromal antigen 2 (BST2) from sites of viral assembly. J Biol Chem 290:10919–10933. https://doi.org/10.1074/jbc.M114.630095.
51. Leitner T, Korber B, Daniels M, Calef C, Foley B. 2005. HIV-1 subtype and circulating recombinant form (CRF) reference sequences, p 41–48. *In* Leitner T, Foley B, Hahn B, Marx P, McCutchan F, Mellors JW, Wolinski A, Korber B (ed), HIV sequence compendium 2005. Los Alamos National Laboratory, Los Alamos, NM.
52. Bell CM, Connell BJ, Capovilla A, Venter WD, Stevens WS, Papathanasopoulos MA. 2007. Molecular characterization of the HIV type 1 subtype C accessory genes vif, vpr, and vpu. AIDS Res Hum Retroviruses 23:322–330. https://doi.org/10.1089/aid.2006.0181.
53. McCormick-Davis C, Dalton SB, Singh DK, Stephens EB. 2000. Comparison of Vpu sequences from diverse geographical isolates of HIV type 1 identifies the presence of highly variable domains, additional invariant amino acids, and a signature sequence motif common to subtype C isolates. AIDS Res Hum Retroviruses 16:1089–1095. https://doi.org/10.1089/08892220050075363.
54. Ndung'u T, Renjifo B, Essex M. 2001. Construction and analysis of an infectious human Immunodeficiency virus type 1 subtype C molecular clone. J Virol 75:4964–4972. https://doi.org/10.1128/JVI.75.11.4964-4972.2001.
55. Long EM, Rainwater SM, Lavreys L, Mandaliya K, Overbaugh J. 2002. HIV type 1 variants transmitted to women in Kenya require the CCR5 coreceptor for entry, regardless of the genetic complexity of the infecting virus. AIDS Res Hum Retroviruses 18:567–576. https://doi.org/10.1089/088922202753747914.
56. Blish CA, Jalalian-Lechak Z, Rainwater S, Nguyen MA, Dogan OC, Overbaugh J. 2009. Cross-subtype neutralization sensitivity despite monoclonal antibody resistance among early subtype A, C, and D envelope variants of human immunodeficiency virus type 1. J Virol 83:7783–7788. https://doi.org/10.1128/JVI.00673-09.
57. Pacyniak E, Gomez ML, Gomez LM, Mulcahy ER, Jackson M, Hout DR, Wisdom BJ, Stephens EB. 2005. Identification of a region within the cytoplasmic domain of the subtype B Vpu protein of human immunodeficiency virus type 1 (HIV-1) that is responsible for retention in the Golgi complex and its absence in the Vpu protein from a subtype C HIV-1. AIDS Res Hum Retroviruses 21:379–394. https://doi.org/10.1089/aid.2005.21.379.
58. Ruiz A, Hill MS, Schmitt K, Guatelli J, Stephens EB. 2008. Requirements of the membrane proximal tyrosine and dileucine-based sorting signals for efficient transport of the subtype C Vpu protein to the plasma membrane and in virus release. Virology 378:58–68. https://doi.org/10.1016/j.virol.2008.05.022.
59. Dell'Angelica EC. 2001. Clathrin-binding proteins: got a motif? Join the network! Trends Cell Biol 11:315–318. https://doi.org/10.1016/S0962-8924(01)02043-8.
60. Richard J, Prevost J, von Bredow B, Ding S, Brassard N, Medjahed H, Coutu M, Melillo B, Bibollet-Ruche F, Hahn BH, Kaufmann DE, Smith AB, III, Sodroski J, Sauter D, Kirchhoff F, Gee K, Neil SJ, Evans DT, Finzi A. 2017. BST-2 expression modulates small CD4-mimetic sensitization of HIV-1-infected cells to antibody-dependent cellular cytotoxicity. J Virol 91:e00219-17. https://doi.org/10.1128/JVI.00219-17.
61. Arias JF, Heyer LN, von Bredow B, Weisgrau KL, Moldt B, Burton DR, Rakasz EG, Evans DT. 2014. Tetherin antagonism by Vpu protects HIV-infected cells from antibody-dependent cell-mediated cytotoxicity. Proc Natl Acad Sci U S A 111:6425–6430. https://doi.org/10.1073/pnas.1321507111.
62. Alvarez RA, Hamlin RE, Monroe A, Moldt B, Hotta MT, Rodriguez Caprio G, Fierer DS, Simon V, Chen BK. 2014. HIV-1 Vpu antagonism of tetherin inhibits antibody-dependent cellular cytotoxic responses by natural killer cells. J Virol 88:6031–6046. https://doi.org/10.1128/JVI.00449-14.
63. Pujol FM, Laketa V, Schmidt F, Mukenhirn M, Muller B, Boulant S, Grimm D, Keppler OT, Fackler OT. 2016. HIV-1 Vpu antagonizes CD317/tetherin by adaptor protein-1-mediated exclusion from virus assembly sites. J Virol 90:6709–6723. https://doi.org/10.1128/JVI.00504-16.
64. Bachle SM, Sauter D, Sibitz S, Sandberg JK, Kirchhoff F, Moll M. 2015. Involvement of a C-terminal motif in the interference of primate lentiviral Vpu proteins with CD1d-mediated antigen presentation. Sci Rep 5:9675. https://doi.org/10.1038/srep09675.